# Identification and Elimination of Instabilities During Simulation of Highly Stiff Vehicle Electrical Power System Models

Robert Weber<sup>1</sup> Staša Gejo<sup>1</sup> Rainer Gehring<sup>1</sup> Lars Mikelsons<sup>2</sup>

<sup>1</sup>BMW Group, Germany, {robert.we.weber, stasa.gejo, rainer.gehring}@bmw.de <sup>2</sup>Chair for Mechatronics, University of Augsburg, Germany, lars.mikelsons@informatik.uni-augsburg.de

#### **Abstract**

In vehicle electrical power system simulations, reliable models are required, especially for critical use cases such as inrush currents, short circuits, and load dump scenarios. These switching scenarios involve rapid changes in resistance and result in stiff models due to the fast dynamics. Instabilities are observed immediately after switching, highlighting significant numerical challenges. In this study, we investigate the origins of these inaccuracies and propose robust solutions through improved electrical models and advanced numerical integration techniques with optimized error tolerance settings. The suggested decoupling approach employs physical and signal filtering techniques to replace the variable resistor used to simulate the fuse switching process. The nominal value strategy involves establishing an appropriate baseline value. The methods discussed yield stable and accurate simulations when implemented with appropriately adapted modelspecific parameterizations.

Keywords: stiff model simulation, vehicle electrical system simulation, numerical instabilities, decoupling method, nominal value

#### 1 Introduction

The importance of the electrical power system for vehicle operation and safety is ever-increasing, due to the growing complexity and reliance on integrated assistance and safety functions in modern vehicles. As the automotive industry moves towards increased automated and autonomous driving functions, new challenges arise in achieving functional safety (Schwimmbeck, Buchner, and Herzog 2018).

New electronic fuses play a vital role in ensuring the safe operation of power distribution units by implementing protection mechanisms like overcurrent, overtemperature, undervoltage, and wire protection algorithms. These functions guarantee the reliable supply of safety-critical consumers even in error conditions, through the quick and selective isolation of faults (Baumann, Abouzari, et al. 2023). To ensure the reliability and availability of these safety-critical systems, it is crucial to perform highly dynamic simulation tests, such as inrush current, short circuit, and load dump scenarios, visualized in Figure 1.

Short circuit tests are performed adjacent to the load to evaluate the fuse's fault isolation capability. Moreover, inrush current tests assess the immediate electrical response upon fuse closure, while load dump scenarios simulate the transient overvoltage conditions, resulting from the abrupt load disconnection via the fuse.

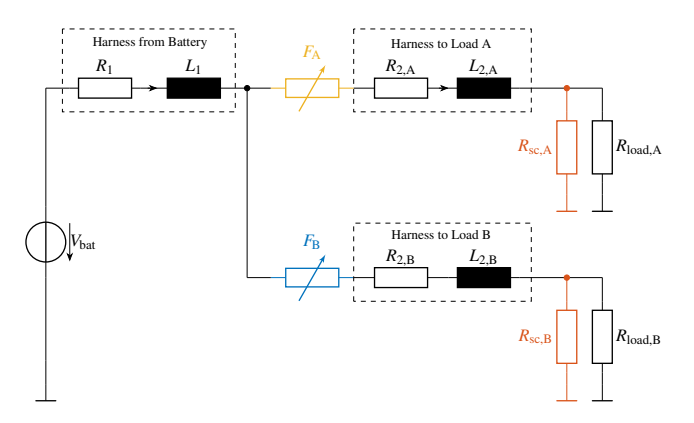


**Figure 1.** Simplified model of the vehicle electrical power system visualizing the different test cases: short circuit scenarios via small resistors  $R_{\rm sc,A}$  and  $R_{\rm sc,B}$  (marked in orange) connected to ground, load dump scenario by opening fuse  $F_{\rm A}$  (marked in yellow) and closing fuse  $F_{\rm B}$  for the inrush current scenario (marked in blue).

Evaluating the vehicle electrical power system functionality and simulation results is challenging, as discontinuities and steep gradients can lead to numerical artifacts. The time constants of the circuit elements can vary by several orders of magnitude, so the effective time constant changes as the resistance varies during switching. This change in resistance alters the dynamic behavior of the system, which is why it is considered *stiff*. Highly stiff or hybrid stiff systems – i.e., systems with discontinuities and Boolean functions that alter the mathematical model description – can be computationally expensive to solve. Moreover, their results are sensitive to solver settings, which poses a challenge for safety-related investigations (Liu, Felgner, and Frey 2010).

One of the common problems encountered during the simulation of electronic fuses in vehicle electrical systems is the appearance of deviations from a physically correct behavior. These deviations manifest as uneven sawtooth disturbances in the voltage across the fuse or as a single exaggerated spike caused by integration instability, rather

than by physical phenomena. Such voltage behavior can be critical, as it serves as an input for additional components – such as the diodes connected in parallel with the fuse. Diodes alone may pose numerical challenges, and an unstable voltage input can introduce further complications in the numerical simulation. They are employed as a protective measure to limit the voltage across the fuse. Furthermore, the fuse trigger limits can be incorrectly breached, leading to erroneous simulation model behavior (e.g. undervoltage). All these aspects can have a significant negative impact on the numerical stability and functionality of simulation models. The goal of this work was to find the sources of numerical instabilities in these models and to resolve them by means of physical remodeling or by using more advanced integrator settings.

Chapter 2 discusses the properties of the vehicle electrical power system. Chapter 3 characterizes the non-physical numerical artifacts observed in the simulation, examining their causes and consequences. The practical remodeling approaches are presented and discussed in Chapter 4. Integrator settings as well as the error estimation and tolerance, and their effect on the simulation results are covered in Chapter 5. Lastly, Chapter 6 compares the presented methods applied in two different models and sets the ground for future research and improvements.

### 2 Vehicular Electrical Power System Simulation Models

The models examined in this chapter represent key elements of vehicular power systems, consisting of voltage and current sources, variable resistors, and signal conditioning circuits, used to represent the behavior of switched electronic fuses and other protective devices. These models can be used to capture transient effects previously mentioned under inrush currents, short-circuit events, and load dump conditions, covering a broad range of time constants.

Such highly dynamic systems are usually also *stiff*. There is no unique definition of stiffness; however, according to Lambert (1992) and Cellier and Kofman (2006), there are several criteria which can be used to recognize or define a stiff system. The two criteria important for this work are:

- Statement A: "A linear constant coefficient system is stiff if all of its eigenvalues have negative real part and the stiffness ratio is large."
- Statement B: "A system is said to be stiff in a given interval of time if in that interval the neighboring solution curves approach the solution curve at a rate which is very large in comparison with the rate at which the solution varies in that interval."

According to Statement A, a linear electrical system is considered stiff if the real parts of its eigenvalues differ by several orders of magnitude.

Let us look at an example of an interconnected load model, consisting of a line, load input impedance, and closed switch found in Baumann, Weissinger, and Herzog (2019), shown in Figure 2. Its eigenvalues are  $\lambda =$  $\{-1.43 \cdot 10^{10}, -5.88 \cdot 10^4 \pm j \cdot 4.01 \cdot 10^4, -4.45 \cdot 10^{-3}\},\$ whose ratios of real parts go from 10<sup>6</sup> up to 10<sup>13</sup>. This type of circuit is omnipresent in the vehicle electrical power system, though in slightly varying input impedance topologies but with similar order of magnitude of its parameters. These circuits connect numerous consumers (small motorized components, heaters, wipers, and ventilators) with the supply, converters, and power distributors. System stiffness arises from the input impedance, cable, and parasitic effects in complex components which can create states with vastly different time constants (referring to Statement B). Additionally, fuse switching causes the total resistance value to change, amplifying variations in time constants and eigenvalues over time. Consequently, this alteration introduces a change in the stiffness of the system. Another cause of numerical issues and instabilities can be discontinuities, as well as nonlinear components and signals.

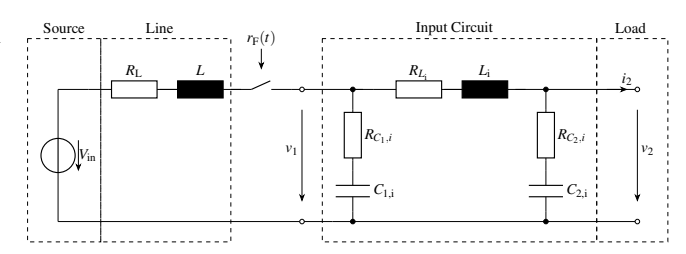


**Figure 2.** Interconnected load model adapted from Baumann, Weissinger, and Herzog (2019).

The problem of numerical integration for stiff problems has persisted for decades, and no integration method is able to solve every stiff problem. Various integrators can be used for stiff applications, such as Radau, LSO-DAR, CVODE, and DASSL, as well as a whole range of ESDIRK methods (Liu, Felgner, and Frey 2010; Cohen, Hindmarsh, and Dubois 1996; Blom et al. 2016). These integrators can be classified as either single-step methods, which rely only on the current integration step, or multistep methods, which use several previous steps to compute the next time step. In addition, the methods differ in the order of integration. Four solvers, including DASSL and RADAU IIA, were compared in a stiff system simulation in Liu, Felgner, and Frey (2010), which showed that DASSL had a higher number of calculated points and a higher solver efficiency for a stiff continuous and stiff hybrid model. However, the study showed a lack of accuracy in all compared solvers for the stiff hybrid system. It is important to note that accuracy and efficiency always depend on the simulated model and cannot be generalized. This work will use DASSL for all the models, as it is wellsuited for stiff systems due to its implicit multi-step properties.

### 3 Model Analysis

"Stability" is a broad concept used to define the behavior of a system. *Analytical* stability, in simplified terms, refers to the property of the system to achieve a steady state after a transient or to remain asymptotically bound. On the other hand, the lack of *numerical* stability (Cellier and Kofman 2006), or rather a *discretization* instability (Ardourel and Jebeile 2021), refers to the lack of ability of the system to numerically reproduce the exact solution. The reason for it lies in the small differences between the original differential equation and its implemented discretized version in the applied numerical method. In other words, a system is numerically unstable if, however small the step size is, a significant deviation arises between the exact solution and the numerical solution (Ardourel and Jebeile 2021).

An additional problem of numerical integration is inaccuracy due to round-off, truncation, and accumulation error. Reducing the step size improves the accuracy but also increases the computational cost. A good balance between error and cost can be achieved by the use of variable-step integration algorithms which utilize specific step-size control algorithms. (Cellier and Kofman 2006)

If a variable-step solver is used, the estimated local error at a given simulation step is controlled to satisfy the following condition (*Dymola Full User Manual* 2022):

$$|local error| < tol_{rel} \cdot |x_i| + tol_{abs}$$
 (1)

By default in Dymola, the relative and absolute tolerances of the simulation are equal, reshaping the Equation 1 into Equation 2, where "tol" denotes the available tolerance input in the setup.

$$|local error| < tol \cdot (|x_i| + 1)$$
 (2)

Dymola Full User Manual (2022) roughly defines the relative tolerance as the approximate definition of the "number of expected true digits in the solution". Meaning, if the value of the state x at a time step i is close to zero, the value of absolute tolerance will determine the limits of the local error. The role of the +1 operation in the brackets in Equation 2 and the settings that change its value, affecting the error calculation, will be discussed in Chapter 5.

Consider the example from Figure 3, which is used to examine the instability in the fuse voltage when inductance is present. The resistor  $R_{\text{load}}$  represents a simple resistive load with no input circuit. The fuse is connected to the source and load via wiring harness models. The fuse is modeled as a simplified component that switches off by acting as a variable resistor, with its resistance changing according to the adapted sigmoid function defined in Equation 3. A key element of these simulations is the detailed representation of the resistance change dynamics of the fuse, closely approximating the behavior observed in

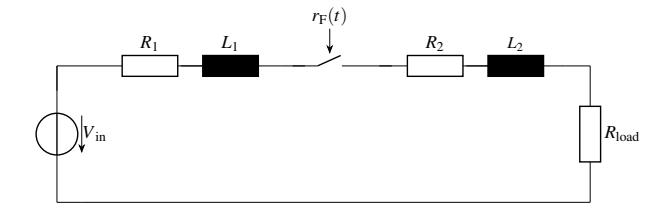


**Figure 3.** A simple circuit used to investigate the fuse voltage instability in the presence of inductance. The circuit comprises a source, a fuse with upstream and downstream wiring harness models, and a simplified load.

the physical fuse. Such modeling provides a more accurate insight into the fuse's effect on the vehicle electrical system.

$$r_{\rm F}(t) = -\frac{R_{\rm F,off}}{1 + e^{k \cdot (t - T_{\rm sw})}} + R_{\rm F,off} + R_{\rm F,on}$$
 (3)

The switching time  $T_{\rm sw}$  is the defined time instant where the switch between the "on" and "off" states is at a halfway point; k is the rate of change of the exponential element. The "on" and "off" state resistances are  $R_{\rm F,on}=1\,{\rm m}\Omega$  and  $R_{\rm F,off}=10\,{\rm M}\Omega$ . The off state is chosen to approximate "open-circuit" conditions. The simulation is run with the DASSL solver, using different tolerance values ranging from  $10^{-5}$  to  $10^{-8}$ . The artifact visible in fuse voltage, as illustrated in Figure 4, indicates a numerical error rather than an actual system response.

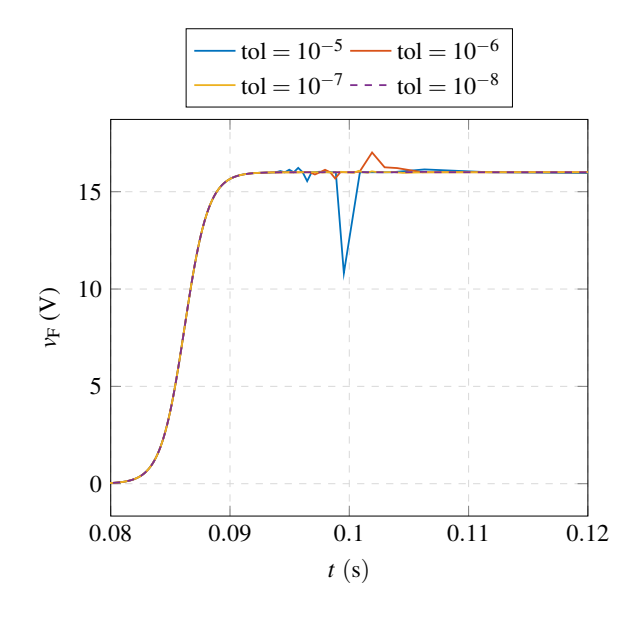


**Figure 4.** Instability in fuse voltage across different relative error tolerance values.

Such a sharp, triangular deviation is not characteristic of the passive electrical elements under a continuous switching function. It is shown to be a consequence of numerical inaccuracy, as reducing the relative error tolerance by one order of magnitude to  $10^{-8}$  eliminates any visible disturbance in the signal. In order to see what causes such

a spike after the voltage transition seemingly ends, an additional plot was generated that marks every simulation step, as depicted in Figure 5.

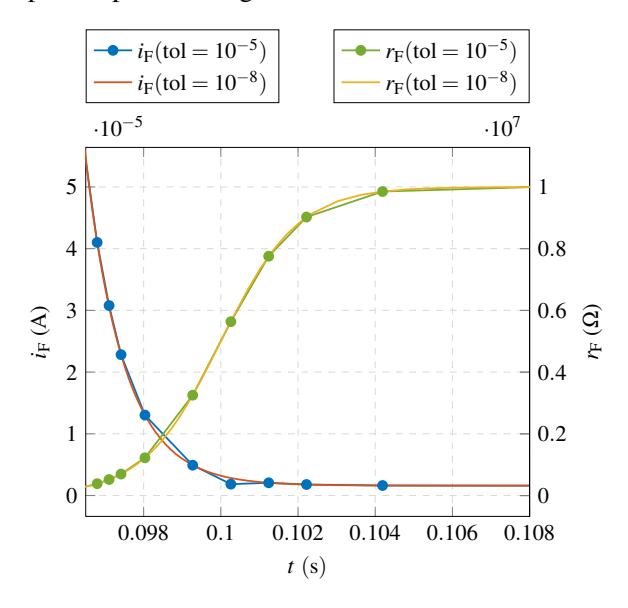


**Figure 5.** Current and resistance of the variable resistor across different relative tolerance values are plotted. Additionally, the solver steps for tol =  $10^{-5}$  are marked.

As the fuse resistance keeps rising and reaching  $5 M\Omega$ , the voltage approaches the value of the source voltage  $V_{\rm in} = 16 \, \rm V$ . The "off" current is already in the order of microamperes, which means that the relative error tolerance is insufficient to maintain calculation accuracy. Further calculations in the integration algorithm for the ODE problem involve both very small (µA) and very large quantities (M $\Omega$ ). However, the disparity in the orders of magnitude between these quantities induces a significant error amplification, ultimately resulting in voltage deviations in the order of several volts. This deviation can be seen in the fuse current plot, where  $i_F$  is a result of simulation using relative tolerances of tol =  $10^{-5}$  and tol =  $10^{-8}$ . At time t = 0.100256 s, the current value at tol =  $10^{-5}$  is deviating from the "expected" current at tol =  $10^{-8}$ , leading to an error magnification to the voltage level. Using a smaller value for the relative tolerance helps keep the step size small enough to avoid any error escalation. Only at  $tol = 10^{-8}$  is the inaccuracy not present.

Equations 4 to 11 present the causal system of equations for the model generated by Dymola. The integration inaccuracy is evident in the voltage signals of both inductors  $(v_{L_1}, v_{L_2})$  as well as in the voltage across the fuse  $(v_{r_{\rm F}})$  in the circuit shown in Figure 3.

When the error occurs in the integration of the differential equation of the current in Equation 9, it is propagated through the calculations of all the voltages, including the negative potential on  $R_1$  in Equation 7. These voltage values are subsequently fed back into the derivative of the current in Equation 9, which can further exacerbate the error.

$$v_{R_2} = L_2 \cdot i \tag{4}$$

$$v_{r_{\rm F}} = r_{\rm F} \cdot i \tag{5}$$

$$v_{R_1} = L_1 \cdot i \tag{6}$$

$$\bar{v_{R_1}} = V_{in} - v_{R_1} \tag{7}$$

$$v_{R_{\text{load}}} = R_{\text{load}} \cdot i \tag{8}$$

$$\frac{\mathrm{d}i}{\mathrm{d}t} = -\frac{1}{L_1 + L_2} (v_{R_2} + v_{r_F} - v_{R_1} + R_{\text{load}})$$
(9)

$$v_{L_1} = L_1 \cdot \frac{\mathrm{d}i}{\mathrm{d}t} \tag{10}$$

$$v_{L_2} = L_2 \cdot \frac{\mathrm{d}i}{\mathrm{d}t} \tag{11}$$

It shall be noted that, although this is a simple example, the same effect can be observed in more complex circuits, e.g. in the model below and generally in the vehicular power system simulations as well. The model developed by Baumann, Abouzari, et al. (2023) is a slightly expanded version of the previously shown model in Figure 3. In this model, additional consumers are added to the single supply line (with one fuse), each equipped with individual input circuits and resistive load elements, as illustrated in Figure 6.

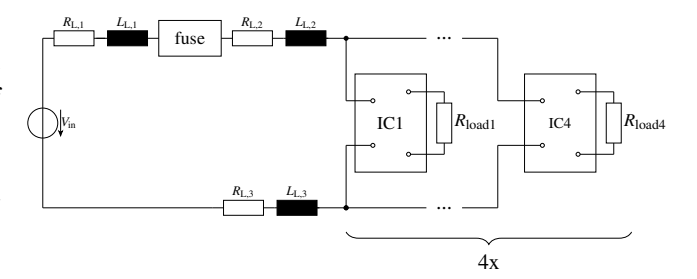


**Figure 6.** Simple multi-load model with a source and one resistive fuse element, interconnected with cables. Each resistive load has an input circuit (IC) block.

This time the fuse variable resistor is controlled with a more advanced dynamic switching function, developed by Baumann, Abouzari, et al. (2023). The fuse is switching the load "off" from the supply at  $t=0.1\,\mathrm{ms}$ . As shown in Figure 7, the numerical accuracy is present even after the significant change in fuse voltage. A very small current and a very large changing resistance are unfavorable for the integration algorithm. When the relative and, consequently, the absolute tolerance of the simulation are reduced, the errors observed in the previous case are resolved.

However, such a low relative tolerance value is too low for the highly stiff large-scale systems required in the design of vehicular electrical systems. It can cause a complete simulation failure during switching or even at the very start of the simulation. Hence, an alternative solution was explored that does not involve a direct limitation of the global relative tolerance.

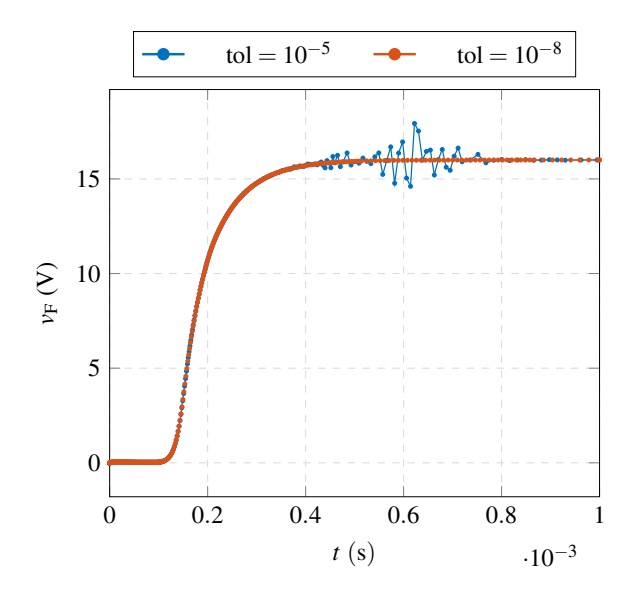


**Figure 7.** Voltage response for  $v_F$  across the fuse at  $tol_{rel} = 10^{-5}$  (default) and  $tol_{rel} = 10^{-8}$ .

# 4 Simulation Approaches for Switched Electronic Fuses

In the following, a signal and a physical filtering approach is proposed to mitigate instability. The variable resistor is remodeled and the circuit is split, yielding an equivalent model referred to as decoupling. This serves as a necessary preparatory step for the implementation of the filtering approaches.

#### 4.1 Decoupling

The main idea behind the decoupling is to use controllable current and voltage sources. This allows for the implementation of a custom control function rather than using a variable resistor. Its resistance directly affects the system matrix and variations in its value modify the system eigenvalues. Therefore, an indirect way of securing the same voltage behavior was required to construct an equivalent system with the use of the closely available physical quantities. Among the decoupled attempts with different source combinations, the best implementation was found in the combination of the controlled current source on the primary (supply) side and a controlled voltage source on the secondary (output or load) side. This configuration is presented in Figure 8.

Equations (12) and (13) were implemented to control the respective sources using the mathematical expression for the desired resistance change of the fuse, the measured secondary current  $\hat{i}_y$  and the measured primary voltage  $\hat{v}_x$ . The measured current from the secondary circuit is fed to the current source on the primary side, ensuring identical conditions as in the original model, whereas the secondary voltage was controlled indirectly via the shown expressions. Voltage was measured between the positive nodes of the two decoupled sides  $v_{xy}$  to obtain the equivalent of

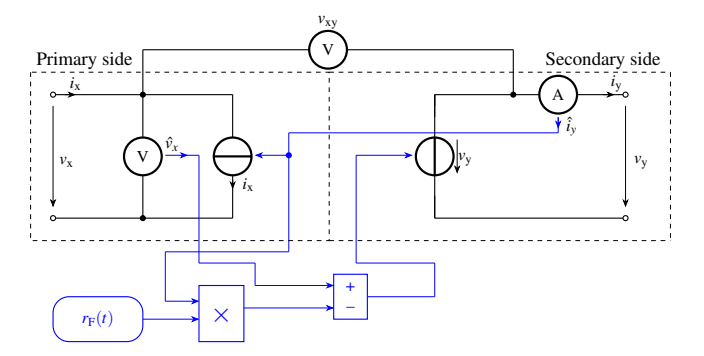


**Figure 8.** Decoupling implemented with a combination of a controlled current and voltage source (CV).

the fuse voltage. The notation CV will be used to denote this implementation in the subsequent text.

$$v_{\mathbf{y}}(t) = \hat{v}_{\mathbf{x}}(t) - \hat{i}_{\mathbf{y}}(t) \cdot r_{\mathbf{F}}(t) \tag{12}$$

$$i_{x}(t) = \hat{i}_{v}(t) \tag{13}$$

An option that was explored as well included two controlled voltage sources (further denoted as VV), whose inputs are shown in Equations (14) to (16).

$$v_{v}(t) = \hat{v}_{x}(t) - \hat{i}_{x}(t) \cdot r_{F}(t) \tag{14}$$

$$v_{x}(t) = \hat{v}_{y}(t) + \hat{i}_{y}(t) \cdot r_{F}(t)$$

$$\tag{15}$$

$$i_{x}(t) = i_{y}(t) \tag{16}$$

This approach has certain disadvantages due to its structure. The most significant problem is the occurrence of a division by zero in one of the differential equations of the simulation model. Therefore, to avoid the division by zero a correction factor is defined to only slightly differ from the original factor in the addition block. However, this very small value in the denominator had a negative impact on the stability of the model. Apart from these VV drawbacks, no other significant differences between the two approaches that could affect the stability of the model were observed.

Since the secondary current is measured and fed to the primary, the sensitive state can be accessed directly. Due to the previous comparison of the two approaches, the decoupled CV was subsequently used for further investigation.

#### 4.2 Signal Filtering

Decoupling the system offers a significant advantage of transforming a purely electrical model into a signal-based switching system. This approach enables modifying the signals for both the controlled signal current on the primary side and the controlled signal voltage on the secondary side. Since it is known that instabilities arise from even minimal inaccuracies in the current, which are amplified by large resistance values, the idea was to smoothen the entry to the controlled signal voltage. This can be achieved by employing a filter, as shown in Figure 9.

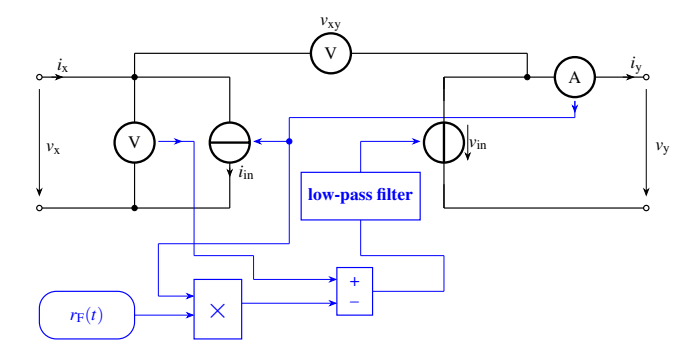


Figure 9. Decoupled model with an integrated low-pass filter.

Such an implementation can achieve a smoother transition during switching operations. When it comes to the primary side, filtering the current directly is neither necessary nor effective, as the current response itself has no evident sawtooth disturbances. Additionally, primary and secondary currents must remain equal, in order to retain the equivalence to the original circuit (Equation 13).

Various strategies can be employed to smoothen the signal input for the secondary voltage source, with a first-order element serving as the simplest form of signal-based filtering (Equation 17).

$$\tau \cdot \frac{y_{\text{filter}}(t)}{\text{d}t} + y_{\text{filter}}(t) = K \cdot u_{\text{filter}}(t)$$
 (17)

It is crucial to have a precise understanding of the expected voltage behavior in the circuit before implementing any filters to avoid suppressing significant electrical effects. Additionally, it must be noted that such components influence the system dynamics by introducing a delay and altering the signal's response based on the chosen time constant. It is advantageous to select a very small time constant (e.g.,  $\tau < 10^{-7}$  s) to minimize switching delays and preserve the original electrical characteristics of the signal. The effects of different time constants are discussed in more detail in Chapter 6. The preset gain factor should be set to K = 1.

#### 4.3 Physical Filtering

In addition to the previously introduced signal filter, a physical filter approach is presented. The most promising variant included the RC branch parallel to the controlled sources and an additional inductor on the secondary side. This configuration is illustrated in Figure 10.

**Table 1.** Parameter values used in the decoupled CV with inaccuracy compensation.

Primary side		Secondary side		
$R_{\text{CV}_1}$	$C_{\mathrm{CV}_1}$	$R_{\mathrm{CV}_2}$	$C_{\mathrm{CV}_2}$	$L_{\rm CV}$
$10^4 \Omega$	10 <sup>-9</sup> F	$10^4 \Omega$	10 <sup>-9</sup> F	$10^{-9}{\rm H}$

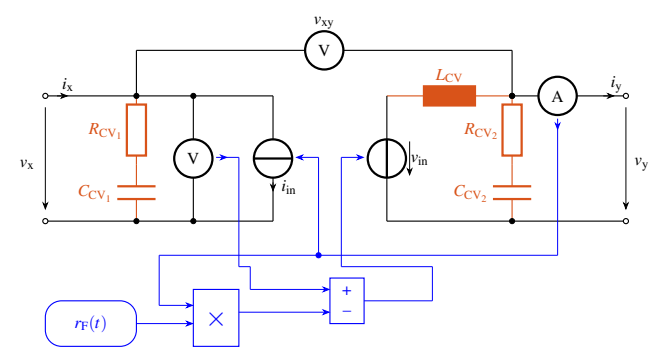


**Figure 10.** Decoupled model with an implemented physical filter approach. The components needed for the filter are highlighted in orange.

This circuit has shown the ability to compensate the numerical error and provide accurate results for the example in Figure 11. The parameters of the additional circuit elements are set to very high resistance values and very low inductance and capacitance values, so as to avoid introducing undesired dynamics into the system. A parametrization example is shown in Table 1.

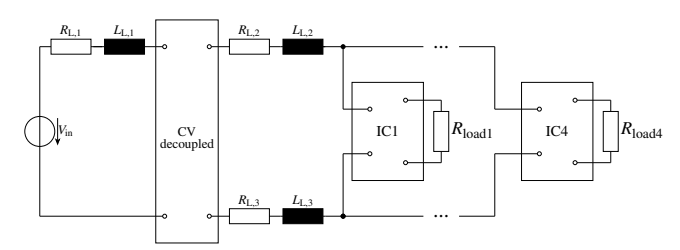


Figure 11. Power system model with decoupled block.

When this implementation is applied to the simplified system with multiple loads with their input circuits, the behavior was stable and accurate. However, if the circuit tends to be predominantly inductive, the shown solution still exhibits inaccuracies. One such example is the small model from Figure 3. Its inductive characteristic causes numerical instability with every possible RC and RLC combination, except in the case with the RC branch only on the secondary side, without an inductor, where the instability is only reduced but not eliminated. Since the RLC components of the physical approach may also represent parasitic effects of the wiring harness, it is possible to investigate whether a more detailed modeling of the wiring harness could lead to a more accurate simulation and reduce instabilities. This could be addressed in future research.

## 5 Elimination of Instabilities by Focusing on the Absolute Tolerance

A *nominal* value indicates the magnitude of a specific state and influences the absolute tolerance. This nominal value is specified in the textual description of the component (*Modelica - Language Specification* 2023).

Listing 1 shows an example in which the current i of an inductor is assigned a nominal value of  $10^{-4}$ .

#### Listing 1. Nominal value definition for a component

L2(i(nominal=1e-4), L=0.75e-6)

Equation 18 demonstrates how error tolerance is effectively distributed using this setting. If the value of the state itself is higher than the defined nominal value, the relative tolerance will dominate the error calculation. Conversely, a higher nominal value shifts the dominance toward the absolute tolerance. But what does it mean in practice?

$$|local error| < tol \cdot (|x_i| + nominal(x_i))$$
 (18)

"A simple way of understanding tolerance is that the relative tolerance sets the number of significant digits to be calculated using:

significant digits = 
$$-\log_{10}(\text{tol})$$
,

(when  $|x_i|$  is larger than the nominal value). And the absolute tolerance sets the number of decimal places:

decimal places = 
$$-\log_{10}(\text{tol} \cdot \text{nominal}(x_i))$$
,

(when  $|x_i|$  is less than the nominal value)" (Fish 2019).

Therefore, it is desirable to use a nominal value of the same order of magnitude as the lower value of the state in which the inaccuracy occurs. Decimal places are used for large values and significant figures for very small ones. It ensures that the step size remains sufficiently small for precise calculations when the state falls below the nominal. This is a crucial point in these switching models because exactly when the current becomes too small for the integrator to keep the accuracy, the large resistance comes into play. This way, the strict accuracy mode is "turned on" only when the state is below the nominal value. Otherwise, the system follows the relative tolerance constraints.

An investigation of the small model in Figure 3 with preset relative tolerance of  $10^{-5}$  reveals that defining an appropriate nominal value for the state leads to immense improvements in the voltage characteristics. This change is illustrated at the bottom of Figure 12.

The simulation analysis performed in Dymola provided access to information on integrator order, step size, and various error indicators and markers. In the upper plot of Figure 12, this small example shows that using the nominal setting (dashed red) results in an extended period of reduced step size compared to the default (dashed blue), thereby enabling more accurate calculations at the end of the switching period. This change is reflected in the integration order remaining at higher values over that extended duration. The step size is reduced as a consequence of more frequent step rejections compared to the simulation with the default settings, as shown by the dots in Figure 12.

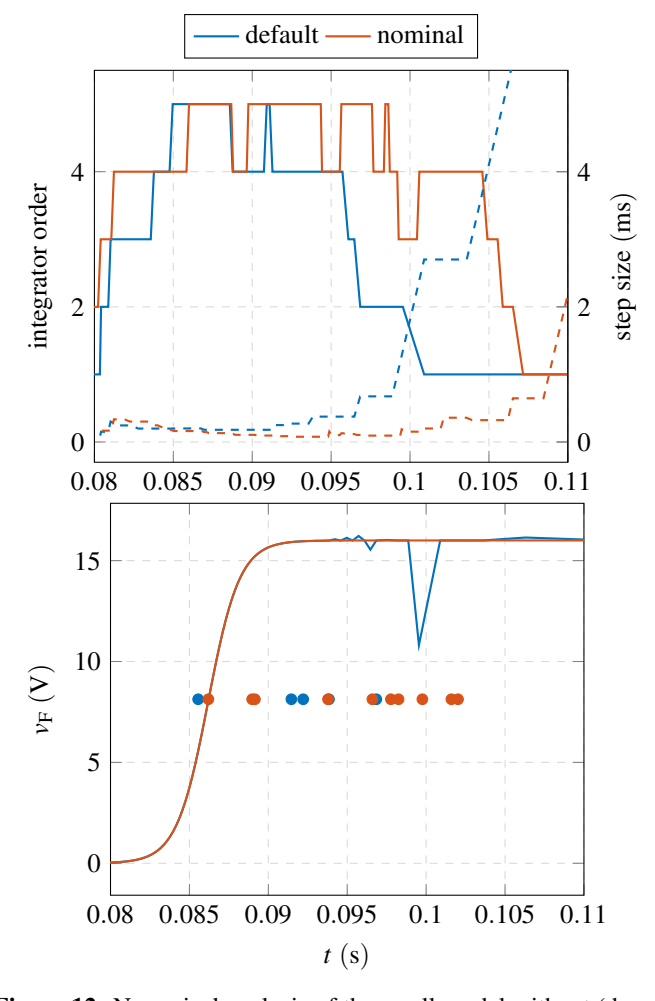


**Figure 12.** Numerical analysis of the small model without (default, nominal = 1) and with a nominal value of  $10^{-4}$ . The upper plot shows the integration order in full line and step size comparison in dashed. The plot below depicts the change in fuse voltage as well as the solver rejected steps as full dots.

#### 6 Results and Discussion

To evaluate the performance of these approaches, two simulations are presented. Firstly, the results from the small-scale power system model are shown, followed by those from a large-scale simulation. Finally, the similarities and differences between the results of these approaches are compared.

# 6.1 Small-Scale Power System Simulation Model

This vehicle electrical system model was previously introduced in Figure 6. The model consists of four loads with integrated input circuits, one fuse, and a corresponding wiring harness. The fuse is switched off at  $t=0.1\,\mathrm{ms}$  changing its resistance from  $1\,\mathrm{m}\Omega$  to  $1\,\mathrm{M}\Omega$ . The function describing the change in resistance during switching off was developed by Baumann, Abouzari, et al. (2023). As a consequence of switching the fuse, the voltage over the resistor changes from  $28\,\mathrm{mV}$  to  $16\,\mathrm{V}$ . Preset tolerance of the simulation is  $\mathrm{tol}_{\mathrm{rel}} = 10^{-5}$ .

Figure 13 displays the voltage across the fuse resistor for the default simulation (shown in blue). Additionally, the previously introduced methods for physical filtering (yellow) and signal filtering (violet), as well as the nominal value (orange), are visible. The parameters for the physical filtering are the same as in Table 1. For signal filtering, a time constant of  $\tau=10^{-8}\,\mathrm{s}$  is used. The trace of the default simulation shows instabilities occurring between 0.4 ms and 0.8 ms. These sawtooth disturbances exhibit a maximum voltage deviation from the equilibrium state of 10.71%. As visualized in the zoomed-in area (A) of Figure 13, the simulation results indicate that both filtering approaches and the nominal setting produce identically smooth voltage outputs.

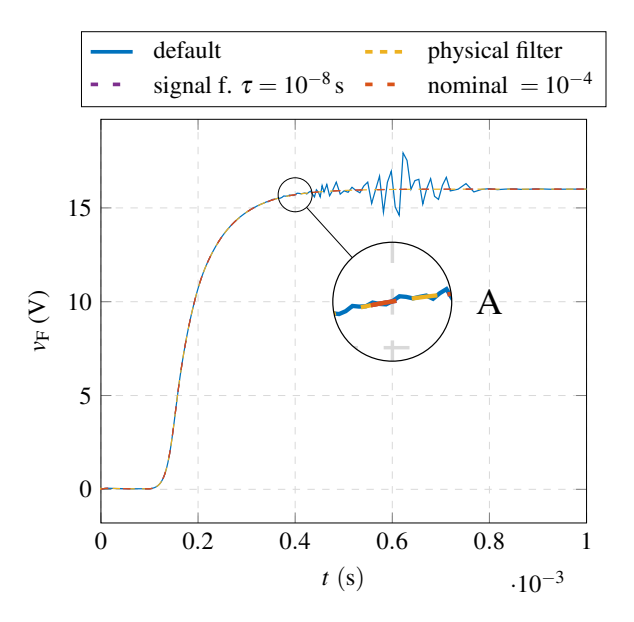


**Figure 13.** Differences in voltage response  $v_F$  across the fuse of the models from Figure 6 and Figure 11 at tol<sub>rel</sub> =  $10^{-5}$  (default).

Further tests have shown that a sufficiently small time constant is  $\tau < 10^{-6}$  s. Since the fuse switches within a time interval of up to  $10^{-5}$  s, the first-order filter can effectively resolve numerical inaccuracies without introducing significant delays in the voltage value. In addition, no negative side effects of the approach can be identified. For the physical approach, adding the RLC and RC branches before and after the variable resistor is also a viable option, yielding results similar to those of the decoupled system with a signal filter. The filter CV models typically do not exhibit a reduced step size compared to the original model, as the filtering elements do not dominate the solver's error estimation. Defining the nominal state value (highlighted in orange) further improves stability at minimal implementation cost, without requiring detailed knowledge of the circuit parameters. The only information necessary to properly set the nominal value is the state that causes numerical disturbances and the precision required to mitigate them. The nominal attribute employs a stricter error tolerance for very small currents. In this example, the approach results in more rejected steps and a smaller step size, as demonstrated in the previously shown example, illustrated in Figure 12.

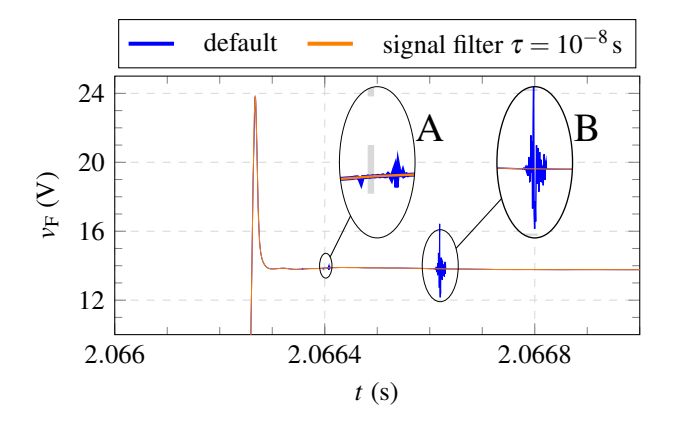
# 6.2 Large-Scale Power System Simulation Model

In the following, the stability of the approaches is evaluated using an electrical power system simulation model developed at BMW. This full model includes all components of the vehicle's electrical consumers, a battery model, the entire wiring harness, and the above-mentioned fuses. In addition, each component contains complex control and monitoring logic. The simulation model is comprised of approximately 1,800 states and about 230,000 equations. In this simulation at t = 2s, a short circuit is initiated, causing the fuse to switch off in accordance with the characteristics described in Chapter 6.1. Despite the preset tolerance ( $tol_{rel} = 10^{-7}$ ) being relatively strict, instabilities are still observed. The fact that we observe such disturbances, even with the tight tolerance, indicates that they occur in almost every power system simulation after switching the fuse. Vice-versa, this contradicts the findings in Figure 5 that instabilities are no longer visible at a preset tolerance of  $tol_{rel} = 10^{-7}$  or stricter. Investigations show that the potential of the deviations is reduced with a tighter tolerance, but it is not guaranteed.

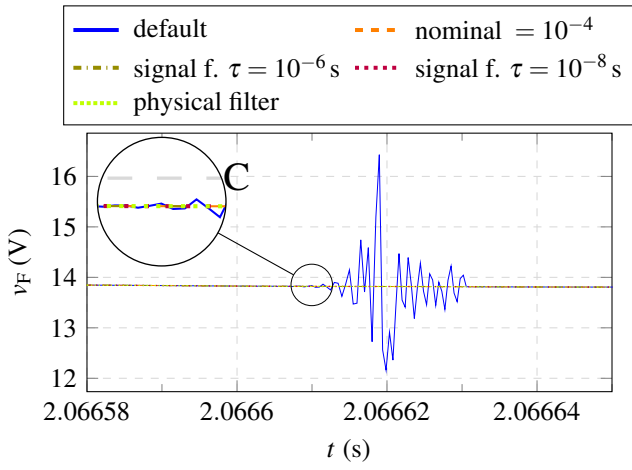
Figure 14 shows the voltage across the fuse resistor, where the same signal filtering technique is applied using two different time constants. Furthermore, the physical approach is presented using the same parameter set as in the initial model described in Table 1, while the nominal approach again employs a value of  $10^{-4}$ . During the switching of the fuse, the voltage across it leads to a voltage peak due to the up- and downstream inductors at time 2.06626s. After the voltage peak, the instabilities occur at 2.06632s and 2.0668s. The maximum deviation is about 15.89% at 2.06662s. As visualized in the zoomed-in areas (A) and (B) in Figure 14a, the characteristic sawtooth disturbances are consistent with those observed in Figure 4.

The signal filter curve ( $\tau=10^{-8}\,\mathrm{s}$ ) demonstrates significant improvements in stability at the time when the inaccuracies in the default simulation model arise. These enhancements occur without any observable change in the electrical system dynamics. Figure 14b presents the zoomed voltage traces and illustrates both the instability characteristics and the results of the implemented approaches. Overall, these simulation results indicate that all introduced and applied methods have effectively eliminated the observed instabilities. Compared to the small model filtering result ( $\tau=10^{-6}\,\mathrm{s}$ ), the large model result ( $\tau=10^{-8}\,\mathrm{s}$ ) also does not exhibit any observable differences after the voltage peak. The effects of different signal filter time constants throughout the complete simulation duration are explored next.

Figure 15 illustrates the same simulation with default settings alongside the signal filtering applied with two dif-



(a) Voltage across the fuse resistor in the large-scale simulation model, comparing the original result with that obtained after applying the filtering approach.



**(b)** Enlarged illustration of the voltage instability across the fuse resistor in a large-scale simulation model and the results for all the approaches presented to eliminate it.

**Figure 14.** Voltage  $v_F$  across the fuse resistor in a large-scale simulation model and the results of the previous introduced approaches.

ferent time constants at  $t = 2 \,\mathrm{s}$ , where a maneuver is initiated. This occurs before the fuse is switched off. In this context, maneuvers refer to vehicle-specific events that change the load on consumers, such as electric power steering. The large-scale simulation shows that a large time constant (definition of "large" relative to the simulation model) leads to oscillations starting at  $t = 2 \,\mathrm{s}$  with a maximum amplitude of 0.21 V. These oscillations can reduce the step size and affect simulation stability. Therefore, the time constant for the filtering approach must be carefully selected.

#### **6.3** Discussion of the Approaches

The implementation of the previously introduced approaches in the two simulation models, which differ significantly in numerical complexity, revealed notable variations in the simulation results. The following discusses these similarities and differences in detail.

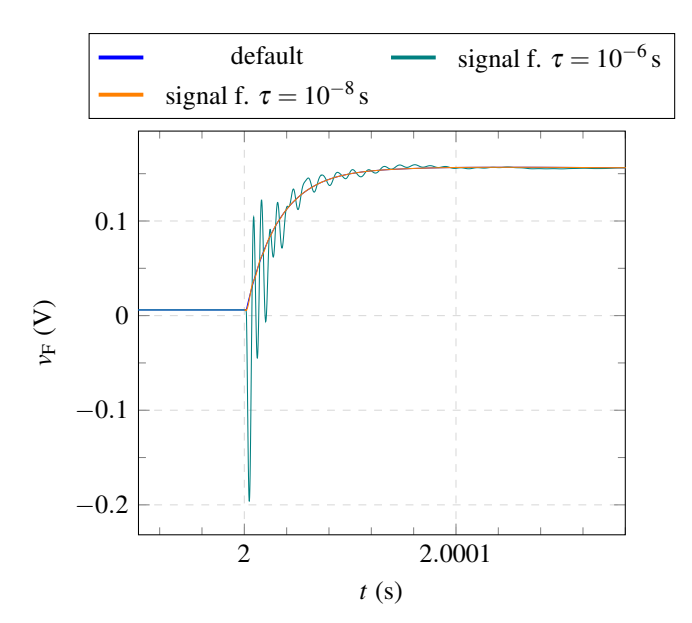


**Figure 15.** Effects of the signal filter with different time constants on the voltage across the fuse resistor at the start of the maneuver in the power system simulation.

#### **6.3.1** Nominal Approach

The nominal approach is attractive due to its straightforward implementation. The simulation results indicate that the instability issues were minimized. Residual ripples may persist, but they typically do not affect simulation stability. The models presented above generally exhibit different behavior with regard to step size. While in the first small-scale simulation the step size is reduced – thereby increasing the simulation time - the large-scale model demonstrates a reduction in simulation time. This effect in the large-scale model is due to the constantly low step size, caused by the remaining states, as well as state and time events of the overall simulation model. As a result, the step size is controlled in a different manner compared to the small-scale model, which can positively affect the simulation time. However, this relationship cannot be determined in advance, as it depends on the individual model and its dynamics. As already mentioned in Chapter 5, the nominal value should be chosen to be of the same order of magnitude as the low state value at which the inaccuracy occurs.

#### **6.3.2** Signal Filtering Approach

By decoupling the system, continuous controllability of the voltage was achieved throughout the simulation. In both models, the implementation of a first-order filter in the voltage path resulted in significant improvements by smoothening the voltage. Importantly, overall simulation performance remained unchanged compared to the original simulation, regardless of the time constant employed. However, large time constants that depend on the simulation model lead to oscillations in both voltage and current. In particular, the current as a state variable further compromises simulation performance and stability. These observations underscore the critical importance of carefully selecting the time constant in the filtering approach. For the demonstrated simulation scenarios, it is recommended to select time constants  $\tau$  between  $10^{-7}$  s and  $10^{-9}$  s. Previous investigations have shown that these values do not cause any noticeable negative effects.

#### 6.3.3 Physical Filtering Approach

Physical filtering is another approach in which different states are integrated before and after the switching element. By using a high resistance and a low capacitance and inductance, instabilities can be eliminated without significantly changing the dominant error or the step size. Both simulation models presented earlier, despite their differences in complexity, have demonstrated that this approach reliably eliminates instabilities. However, the natural delay in the RC circuit in an electrical system can lead to oscillations if the parameters of the components are chosen improperly. When using this approach, it is recommended to employ the previously used parameter values for inductance, resistance, and capacitance. If necessary, these parameters may be reduced by an order of magnitude without compromising stability.

#### 7 Conclusion

A decoupling approach with filters has been introduced as a substitute for the challenging variable resistor element under highly dynamic switching in stiff electrical power system models. On the other hand, an alternative error tolerance setting - nominal - has been explored and compared to the default settings. Decoupling is essential for the signal filtering approach, as it enables the removal of numerical disturbances in a manner analogous to physical filtering. This strategy provides direct access to the perturbed voltage value, which can then be stabilized. Both filter variants successfully achieve their intended purpose without reducing the global relative tolerance. However, the first-order block in the signal variant is considerably simpler to implement. With a sufficiently small time constant, it is also more robust against unwanted voltage instabilities. The application of the physical filtering solution is the more complex method, which involves tuning of the RLC and RC branches to achieve the desired output.

It can be concluded that the fastest and most reliable solution to the problem is the use of the nominal setting in the problematic state, in the magnitude of its low value. However, this method still exhibits a minor error, although in the order of less than a percent of the expected value. The authors advise a thorough understanding of the circuit characteristics, as it is essential to identify the problematic state and subsequently implement a suitable approach.

For future studies, it is recommended to investigate how the various approaches with different parameter sets affect the runtime of the models. Furthermore, it is important to understand the performance implications for different fuses in the power system simulation, given its complexity and size. An alternative approach to achieve the desired voltageswitching characteristic is to use a series-connected controllable voltage source instead of a variable resistor. This configuration replicates the voltage-switching behavior of the electronic fuse rather than relying solely on resistance. Moreover, this approach avoids dependency on the current and high resistance by applying a direct voltage requirement. This solution requires further research and testing to determine potential disadvantages.

#### References

Ardourel, Vincent and Julie Jebeile (2021). "Numerical instability and dynamical systems". In: *European Journal for Philosophy of Science* 11. DOI: 10.1007/s13194-021-00372-7.

Baumann, Martin, Ali Shoar Abouzari, et al. (2023). "Resource-Saving Modeling of an Electronic Fuse in Vehicular Power Systems". English. In: 2023 IEEE Vehicle Power and Propulsion Conference, VPPC 2023 - Proceedings. 2023 IEEE Vehicle Power and Propulsion Conference, VPPC 2023 - Proceedings. Institute of Electrical and Electronics Engineers Inc. DOI: 10.1109/VPPC60535.2023.10403182.

Baumann, Martin, Christoph Weissinger, and Hans-Georg Herzog (2019). "Reducing Transient Disturbances within Automotive Power Systems Through Adapting of Input Circuits". In: 2019 International Conference on Computing, Electronics & Communications Engineering (iCCECE), pp. 214–218. DOI: 10.1109/iCCECE46942.2019.8941977. (Visited on 2024-11-28).

Blom, David S. et al. (2016). "A comparison of Rosenbrock and ESDIRK methods combined with iterative solvers for unsteady compressible flows". In: *Advances in Computational Mathematics* 42.6, pp. 1401–1426. ISSN: 1572-9044. DOI: 10.1007/s10444-016-9468-x.

Cellier, Francois E. and Ernesto Kofman (2006). *Continuous System Simulation*. Springer. ISBN: 978-0-387-26102-7.

Cohen, Scott D., Alan C. Hindmarsh, and Paul F. Dubois (1996).
"CVODE, A Stiff/Nonstiff ODE Solver in C". In: Computer in Physics 10.2, pp. 138–143. ISSN: 0894-1866. DOI: 10.1063/1.4822377.

*Dymola Full User Manual* (2022). Dassault Systèmes AB. Lund, Sweden. URL: https://www.dymola.com/ (visited on 2025-01-05).

Fish, Garron (2019). A closer look at solver tolerance. URL: https://www.claytex.com/tech-blog/a-closer-look-at-solver-tolerance/ (visited on 2024-12-04).

Lambert, J.D. (1992). Numerical Methods for Ordinary Differential Systems: The Initial Value Problem. Wiley. ISBN: 978-0-471-92990-1.

Liu, Liu, Felix Felgner, and Georg Frey (2010). "Comparison of 4 numerical solvers for stiff and hybrid systems simulation".
In: 2010 IEEE 15th Conference on Emerging Technologies & Factory Automation (ETFA 2010), pp. 1–8. DOI: 10.1109/ETFA.2010.5641330.

Modelica - Language Specification (2023). Modelica Association. URL: https://modelica.org (visited on 2025-10-04).

Schwimmbeck, Stefan, Quirin Buchner, and Hans-Georg Herzog (2018). "Evaluation of Short-Circuits in Automotive Power Nets with Different Wire Inductances". In: pp. 1–6. DOI: 10.1109/ESARS-ITEC.2018.8607795.